

Supporting information

A high-performance ambipolar organic field-effect transistors based on a bidirectional π -extended diketopyrrolopyrrole under ambient conditions

Jinfeng Bai,^{a†} Yucun Liu,^{a†} Sangyoong Oh,^b Wenwei Lei,^a Bingzhu Yin^{*a}, Sooyoung Park^{*b} and Yuhe Kan,^{*c}

^a Key Laboratory of Natural Resources of Changbai Mountain & Functional Molecules, Yanbian University, Ministry of Education, Yanji, Jilin 133002, PR China. E-mail: zqcong@ybu.edu.cn; Fax: +86 433 2732456; Tel: +86 433 2732298

^b Director of Center for Supramolecular Optoelectronic Materials (CSOM) Professor of Materials Science & Engineering, Seoul National University, email : parksy@snu.ac.k

^c Jiangsu Province Key Laboratory for Chemistry of Low-Dimensional Materials, School of Chemistry and Chemical Engineering, Huaiyin Normal University, Huaian, China. E-mail: yhkan@yahoo.cn

† These authors contributed equally.

Contents

1. Table

Table S1. Calculated absorption wavelength (nm), oscillator strength (*f*) and transition nature of DPP-2T2P-2DCV

2. Figures

Fig. S1. FT-IR spectrum

Fig. S2. TDA and DSC curves

Fig. S3. Calculated and experimental UV-Vis spectra

Fig. S4. Typical output curves of the OFET devices in air.

Fig. S5. Typical output and transfer curves of the OFET devices in nitrogen

3. Characterization

Fig S6. ^1H NMR spectrum of **DPP-2T2P-2CHO** in CDCl_3 .

Fig S7. ^{13}C NMR spectrum of **DPP-2T2P-2CHO** in CDCl_3 .

Fig. S8. Mass spectrum of **DPP-2T2P-2CHO**.

Fig. S9. ^1H NMR spectrum of **DPP-2T2P-2DCV** in CDCl_3 .

Fig. S10. ^{13}C NMR spectrum of **DPP-2T2P-2DCV** in CDCl_3

Fig. S11. Mass spectrum of **DPP-2T2P-2DCV**.

1. Table

Table S1. Calculated absorption wavelength (nm), oscillator strength (*f*) and transition nature of DPP-2T2P-2DCV at CAM-B3LYP/6-31g* level of theory in chloroform solvent

State	λ_{\max}	<i>f</i>	Main contributions	Character
$S_0 \rightarrow S_1$	595.4	2.0101	HOMO->LUMO (88%)	CT(DPP \rightarrow B-DCV)
$S_0 \rightarrow S_3$	368.3	1.3508	H-2->LUMO (25%), H-1->L+1 (17%), HOMO->L+2 (51%)	CT(DPP \rightarrow B-DCV)
$S_0 \rightarrow S_6$	335.5	0.4475	H-2->LUMO (46%), HOMO->L+2 (32%)	LE($\pi \rightarrow \pi^*$)

2. Figures

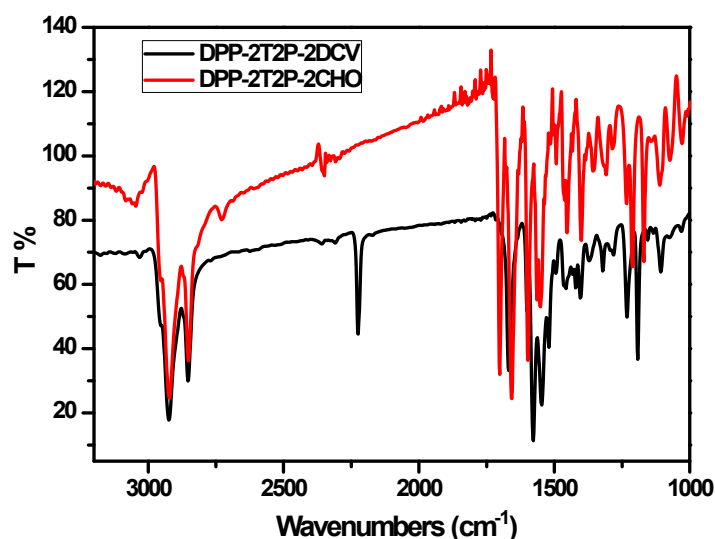


Fig. S1 FT-IR spectrum of **DPP-2T2P-2DCV** and **DPP-2T2P-2CHO**.

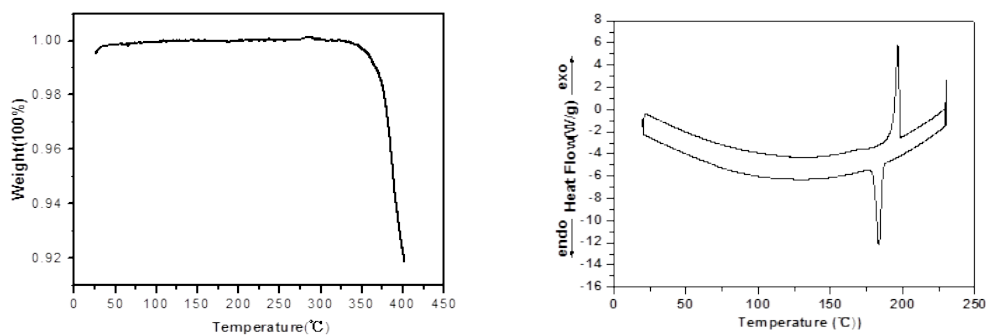


Fig. S2. (left) Thermogravimetric analysis and (right) differential scanning calorimetry curves for **DPP-2T2P-2DCV**.

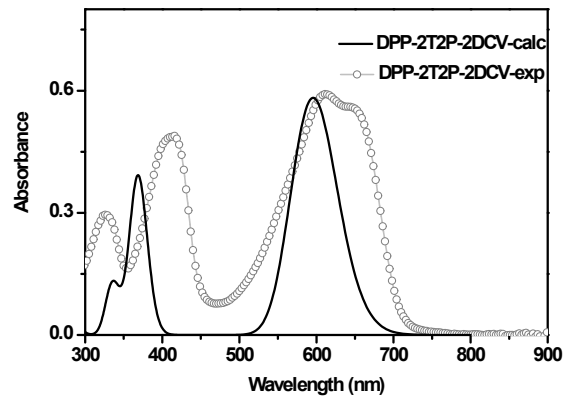


Fig. S3 Calculated absorption spectra of compound I (black solid) compared with experimental spectra (white solid) in acetonitrile.

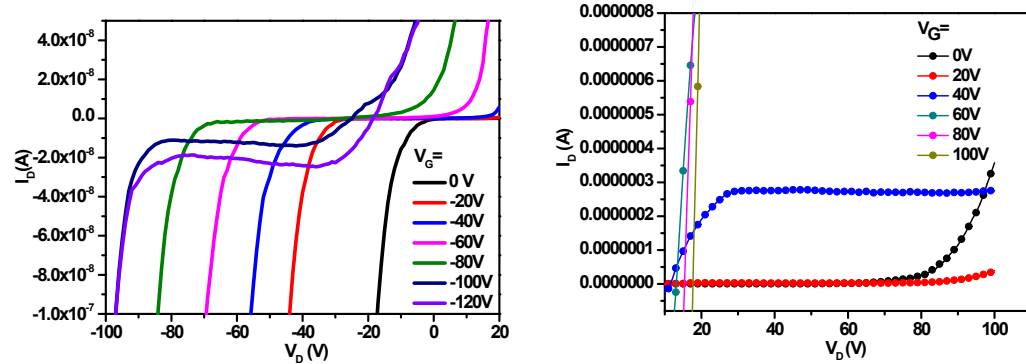
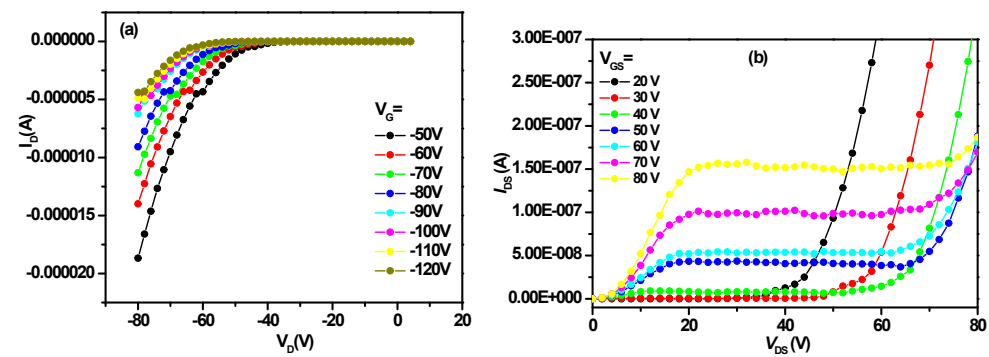


Fig. S4 Typical output curves of the OFET devices in air.



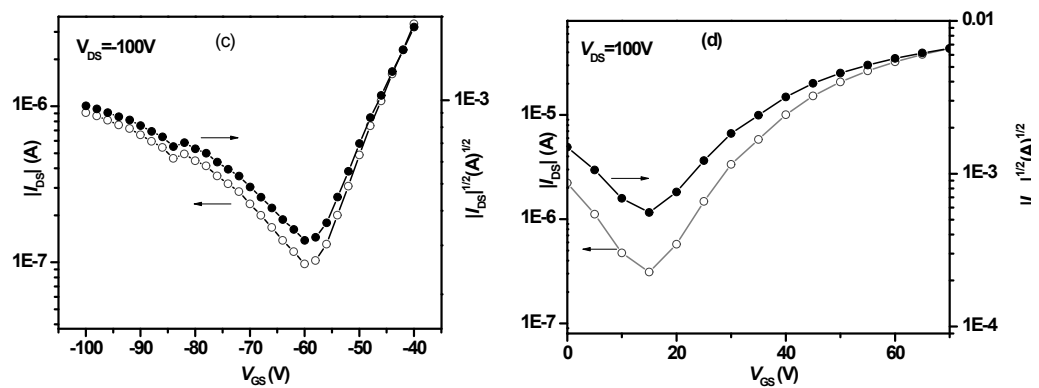


Fig. S5 Typical output (a,b) and transfer (c,d) curves of the OFET devices in nitrogen.

3. Characterization

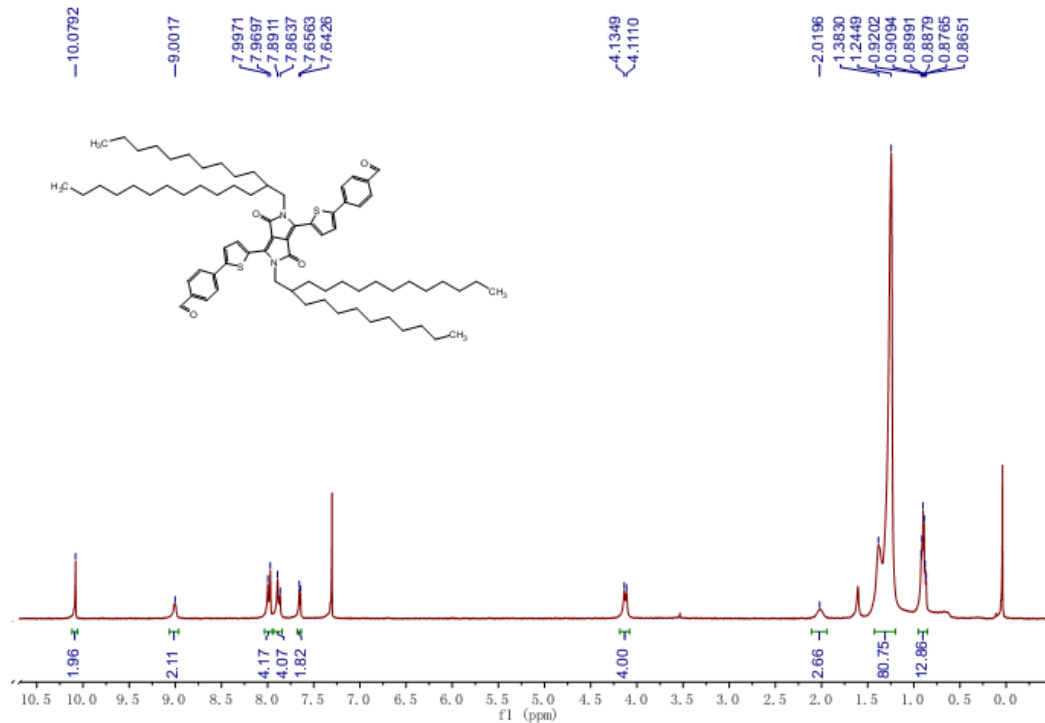


Fig. S6 ^1H NMR spectrum of DPP-2T2P-2CHO in CDCl_3 .

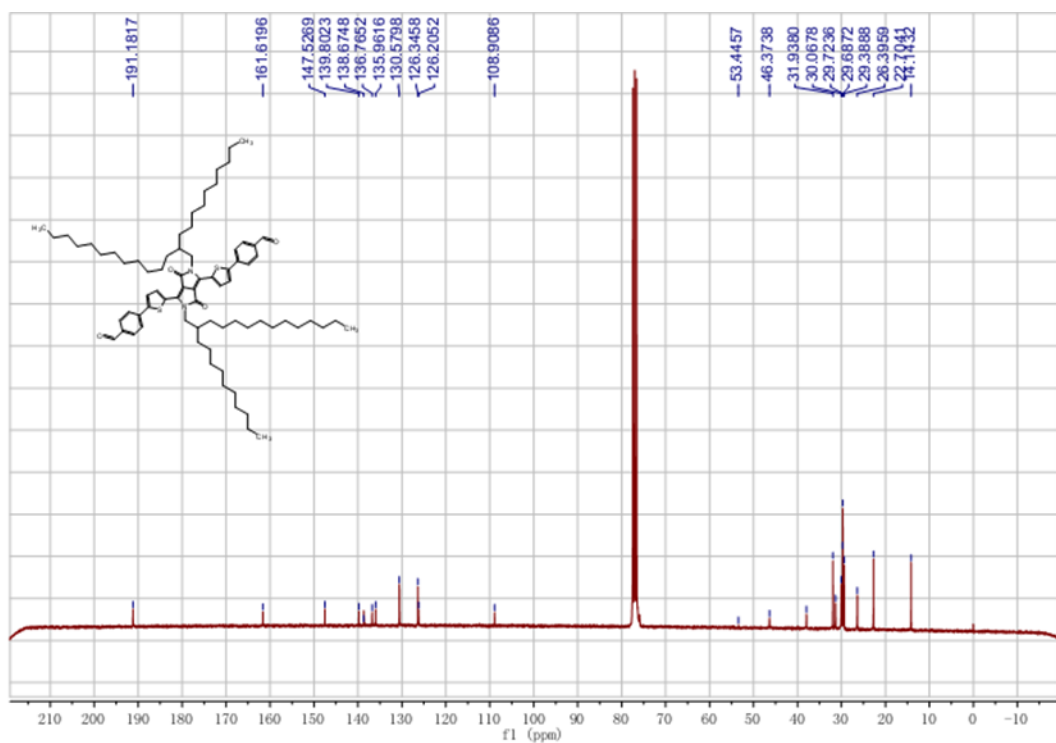


Fig. S7 ^{13}C NMR spectrum of **DPP-2T2P-2CHO** in CDCl_3 .

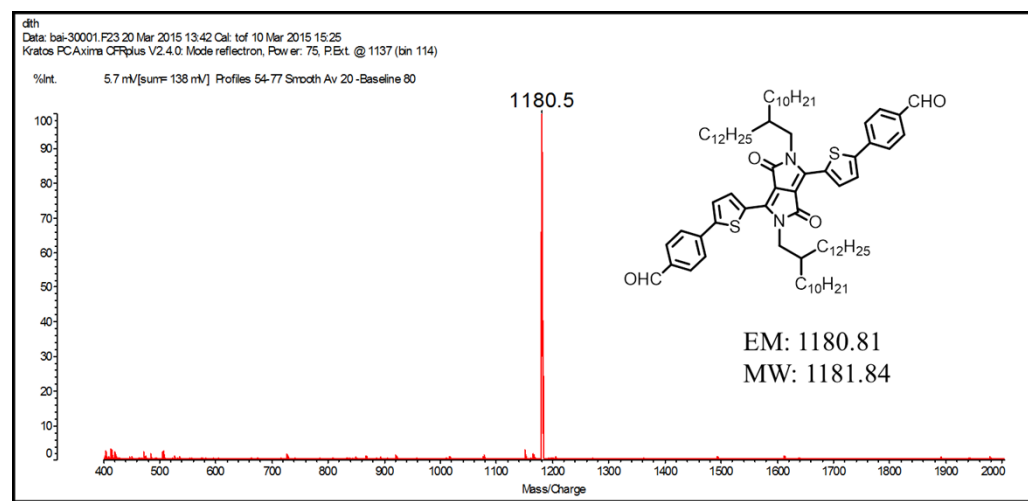


Fig. S8 Mass spectrum of **DPP-2T2P-2CHO**.

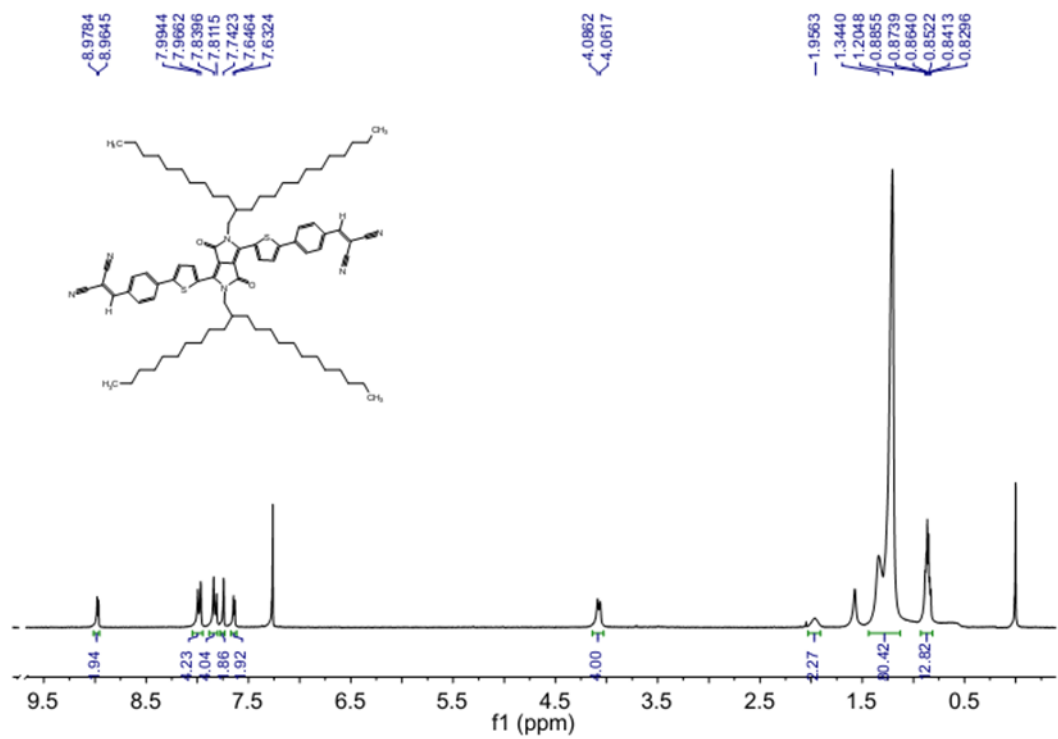


Fig. S9 ^1H NMR spectrum of **DPP-2T2P-2DCV** in CDCl_3 .

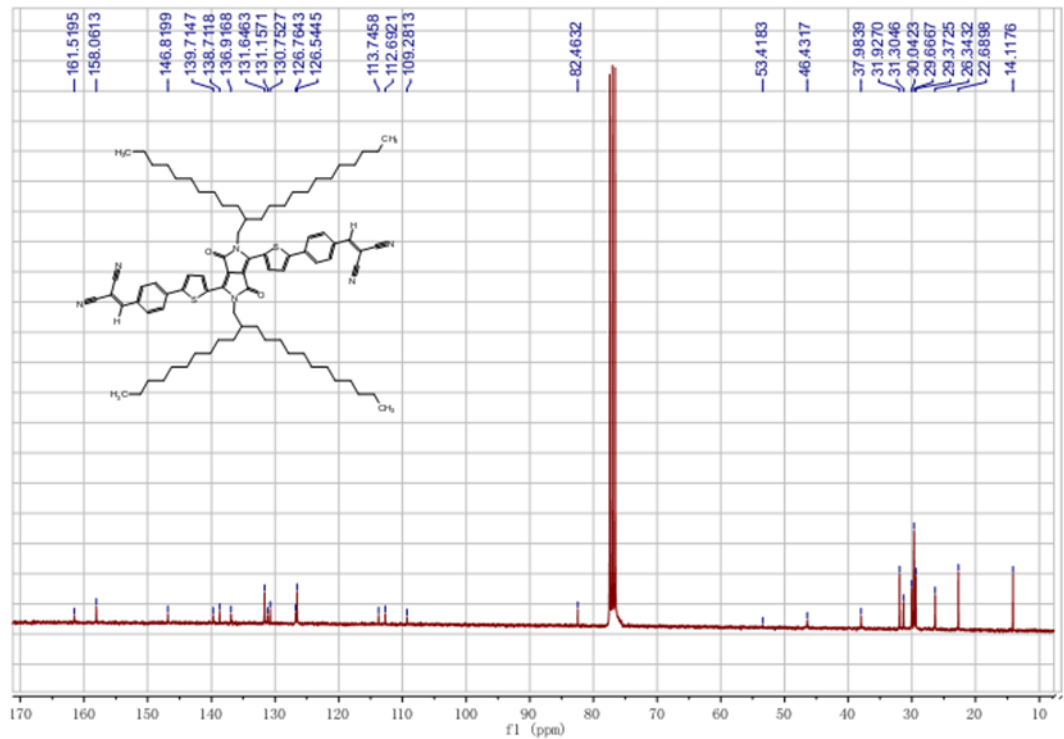


Fig. S10 ^{13}C NMR spectrum of **DPP-2T2P-2DCV** in CDCl_3 .

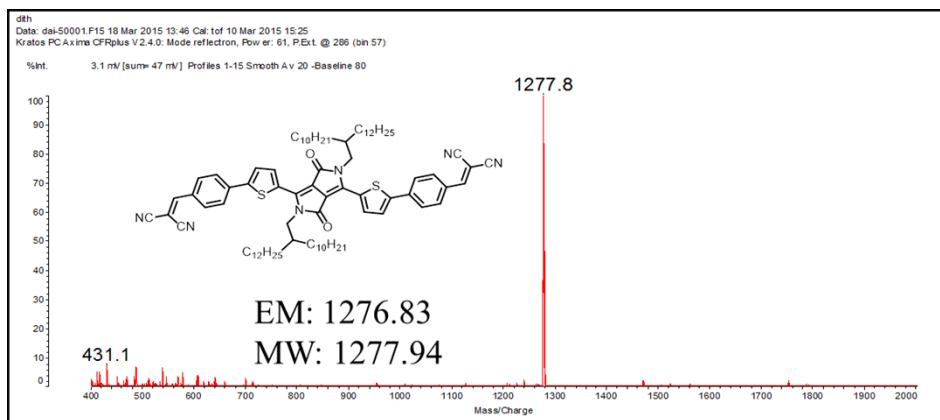


Fig.S11 Mass spectrum of **DPP-2T2P-2DCV**.